

# Reconstructing Power Lines from Images

1<sup>st</sup> Fabio Ganovelli

ISTI

CNR

Pisa, Italy

fabio.ganovelli@isti.cnr.it

2<sup>nd</sup> Luigi Malomo

ISTI

CNR

Pisa, Italy

luigi.malomo@isti.cnr.it

3<sup>rd</sup> Roberto Scopigno

ISTI

CNR

Pisa, Italy

roberto.scopigno@isti.cnr.it

**Abstract**—We present a novel method for 3D reconstruction of overhead power lines from a few images. The solution to this problem has a deep impact over the strategies adopted to monitor the many thousand kilometres of powerlines innervating our countries; currently, the only effective solution is based on the use of high-end laser scanners mounted on drones. The difficulty with image-based 3D reconstruction algorithms is that images of wires of the power lines typically do not have point features to match among different images. We leverage on a few assumptions that can be made on the power lines case and define an ad-hoc strategy for solving the problem. We first use a Structure from Motion algorithm to retrieve the approximate camera poses and then formulate a minimization problem to simultaneously define a 3D wire hypothesis and refine the camera poses so that the projections of that wire are consistent on the supporting images.

**Index Terms**—image based reconstruction, power lines

## I. INTRODUCTION

The ability to reconstruct 3D representations of power lines has a clear impact on the field of asset monitoring (power distribution lines) and risk mitigation. Any segment of a power line is subject to multiple threats. The consumption caused by atmospheric phenomena, the encroaching vegetation, or even just the time passing by may cause interruption on the power transmission and even risk for the people in its close proximity. The most common defects consist of too-low wire sag, because the wire extended too much over its original length, and vegetation infiltration/collision. At the present, 3D reconstruction of power lines is a difficult task and the automation of the reconstruction and monitoring process requires the adoption of high precision time-of-flight scanners mounted on drones [1], [2]. In this setting, the drone flies along the power line and collects dense 3D point clouds of the surroundings, including the wires. Then, the point cloud is processed to extract the shape of the wires and isolate it from the rest of the environment [3], let it be urban [4] or forest areas [5]. Because power lines innervate our countries on a massive scale, monitoring the whole network is an intensive and costly activity.

The much cheaper alternative of 3D reconstruction from images, now extensively used in many other contexts, has not been very successful so far. This is easily explained by the fact that these techniques work if the images contain a

sufficient number of point features to be matched, that is, if there are many point correspondences between partially overlapping images. Unfortunately, wires are very uniform objects that typically do not show such characteristics. Furthermore, wires are kind of *elusive* subjects with respect to image segmentation. If the photographs are taken from above there are innumerable chances for mistaking streets, rivers, and plowed fields with wires. If taken from below the sky may be too bright. If taken from their same height, the projections of multiple wires can cross each other on the image plane.

Like existing approaches to the more general problem of reconstructing wiry objects [6], we rely on the fact that the images contain a sufficient number of features, although off the wires, to enable a SfM method to compute the camera poses accurately. Unfortunately, given the type of scenario, in our case the dataset will be characterized by short baselines compared to the long distances of image features from the camera and, consequently, the pose estimation will be computed with a large error margin. On the other hand, we can exploit specific assumptions that do not hold in the general case of image based reconstruction but they do in the specific case of power lines, that we state in the following:

- 1) The photographs are shot towards a direction of view roughly horizontal and orthogonal to the power lines. This assumption will be used in Section III to simplify the detection of the wires in the images
- 2) The wires of the power line are hung and hence each wire lies on a plane which is orthogonal to the ground. We can rely on IMU mounted on the camera to know the gravity vector. This assumption will be used in Section IV-A to formulate the minimization problem at the core of our solution.

## II. RELATED WORK

Image-based 3D reconstruction has seen a steep evolution in the last decade and can now be considered a mature approach, with a very consistent body of knowledge and many available systems, e.g. Bundler [7], VisualSFM [8], Agisoft Photoscan (<http://www.agisoft.com/>) just to mention a few of them.

The core idea of the *image-based 3D reconstruction* solutions, also called *Structure from Motion (SfM)* methods, is: if we can find a large enough set of feature correspondences among a set of images, then we can both determine the camera poses and the position in 3D space of such features.

Therefore, the whole literature on the subject revolves around techniques to find good feature descriptors (that is as much as possible invariant to geometric transformations), efficient ways to match features between images, and effective bundle adjustment strategies to globally optimize the approximation error. Revising the literature on the general problem is well beyond the scope of this paper (the interested reader can refer to the survey papers [9], [10]), therefore we will limit our references to the works on reconstructing wiry objects with special focus on power lines.

The problem with image-based reconstruction of wiry objects is that they typically do not show point features on the images, which are so essential to any SfM pipeline. A common approach is to generalize the idea of point correspondences to line segment or curve correspondences. 3D segments are used in [11] to improve the point cloud produced by conventional SfM. The first step of the pipeline consists in finding the edges in the images, which in these works is carried out by LSD [12] line detectors. The next step is matching the edges. Given a pair of edges on two images, the candidate 3D edge can be found as the intersection of the projection of the edges in space. Potentially, every pair of 2D edges can make a 3D edge hypothesis. However, correct hypothesis are supported by a higher number of 2D edges/cameras and this fact is used to rank the them with several ranking formulas [11], [13]–[15]. In [6] a method is presented to faithfully reconstruct 3D wire art, that is sculptures make by bending a metal wire. In their approach the detection of the curve is simplified by placing the sculptures on a white background and the work is focused by solving the problem of matching the set of 2D curves correctly by reasoning at junctions of segmented curves.

Curve and segments can also be used to improve the accuracy of the camera poses. In [16] the authors use SfM reconstruction for pose estimation, and then define a global energy function of the camera pose parameters and accounting for the reprojection error of the reconstructed 3D curves. In a subsequent work [17], the same authors lay out the theory for curve-based multiview reconstruction and camera estimation. In [18] the authors used parametric Beziér curves to design a SLAM approach entirely based on curves.

#### Power lines-specific methods

Concerning the specific case of power lines, most of the effort has been focused on correct 2D segmentation, and not to the 3D reconstruction. The problem with power lines is that the context often makes their segmentation difficult. Typically, the images are taken from above and the background may, and in general will, contain roads, plowed fields, and rivers, showing edges with similar characteristics to the power lines and making the distinction difficult. On the other hand, on close views where the power cables are almost parallel and almost straight. These conditions have been harnessed in [19] a pulse coupled neural filter (PCNN) and a variation of the Hough transform are applied. In [20] the problem is tackled by Hough transform and fuzzy c-mean clustering algorithm while in [21] Radon transform and Kalman filter are used to

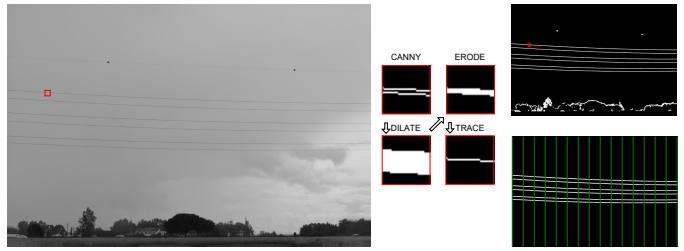


Fig. 1. Steps for segmenting wires from images.

incrementally segment an entire power line. In [22], after an initial classic SfM step, the domain is immersed in a grid of 3D points and each one is back projected onto all images to asses its likability to lie on the power line. Then, power line points are interpolated with the parabola equation. In [23] several software packages are tested for 3D reconstruction from images and a catenary curve is fitted to the few on wire points that are produced.

It should be noted that, although there are several methods using curves for 3D reconstruction and pose estimation, they all work in the assumption that the object of interest is seen by many views with different angles and that there are many edge features. These are not strict assumptions, they generally hold in any image-based acquisition setup. Unfortunately, both these assumptions are broken in the case at hand. In fact we have a set of images of a power line where each image contains only a fraction of it, with some degree of overlaps between images. Furthermore, instead of a large collection of sparse curves or segments we only have the curves to be reconstructed in 3D, which can be as few as a single one.

### III. IMAGE SEGMENTATION AND WIRE COUNTING

Since the images are taken along the power line and looking towards it, the image background typically consists of the sky and the wires stand out clearly, which allow us to use a fairly simple and straightforward segmentation pipeline, illustrated in Figure 1. The first step is to perform a Canny edge extraction. This step typically returns two edges for each wire, one “above” and one “below” the actual wire, where the discontinuities lie. In order to merge them we run a *dilate* filter followed by an *erode* step and finally use a tracking algorithm to return the wires as an ordered sequence of pixel coordinates. The tracking algorithm simply tries move from one white pixel to the next looking only on the right, right and above, and right and below pixels, therefore proceeding *nearly* horizontally. Tracked sequences shorter than 300 pixels are discarded.

Once the segmentation is complete, we proceed to counting the number of wires of the power lines. This is achieved by counting the intersection of vertical lines with the segmented wires at regular step (100 pixels in our experiments) and taking the rounding of the average value.

#### IV. WIRE RECONSTRUCTION AND CAMERA POSE ESTIMATION

We run an SfM algorithm on the set of input images (by using VisualSfM [8], [24]) which produces the camera poses, although in an approximated way, and a set of 3D points. Our target is to find, for each wire segmented in the images, a 3D curve that projects consistently onto all of the images, by allowing small adjustments of the camera poses that we know to be approximated. We first formulate our solution for the case of a single wire and then extend it to the general case.

Since each wire lies in a vertical 3D plane, a 3D wire is uniquely identified as the set of projections of all segmented wires onto such a plane. In other words

$$W(C, \theta) = \bigcup_{\forall h} P_{\theta, C_h}(w_h)$$

where  $W$  is the set of 3D points representing the wire,  $C = \{C_0, \dots, C_M\}$  is the set of extrinsic camera parameters (6 per camera),  $\theta = \{a, b, d\}$  is the set of 3 parameters describing the vertical plane

$$ax + by + d = 0$$

$P_{\theta, C_h}$  is the projection on  $\theta$  of all the 2D points of the segmented wire in the image  $h$  (indicated with  $w_h$ ) using the extrinsic camera parameters  $C_h$ .

We aim at defining an objective function that minimizes the projection error of the wires on the plane  $\theta$ , allowing both the plane and the camera parameters ( $C_h$ ) to change but constraining the reprojection error of the SfM feature points to be below a given threshold. Note that if the camera pose resulting from the SfM were exact, the 3 plane parameters alone would define a solution. Unfortunately, the 3D feature points used for estimating the pose estimation are far away from the camera with respect to the distance between cameras (the baseline in the triangulation process), which means that the orientation and position of the camera as returned by SfM are not very reliable.

In other words, being aware that the camera poses are not accurate, we allow small adjustments in order to make the wire projection coincident on a common plane.

##### A. Wire Projection Error

We define the *wire projection error* as a function of the projection of the segmented 2D wires onto the supporting plane defined by  $\theta$ . We recall that we do not have any point-to-point correspondence between the portion of wire in different image, we only know that their union must be a subset of the wire. Figure 2 illustrates the projection of the same 2D wire from two neighbour cameras on a plane ( $\theta$ ), as seen from each of the two input images (top row) and from a third perspective (bottom). If the plane and the camera parameters were optimized, only one wire should be seen.

We define the error as the sum of a distance function between each point of the first projection and the closest point among all the other projections.

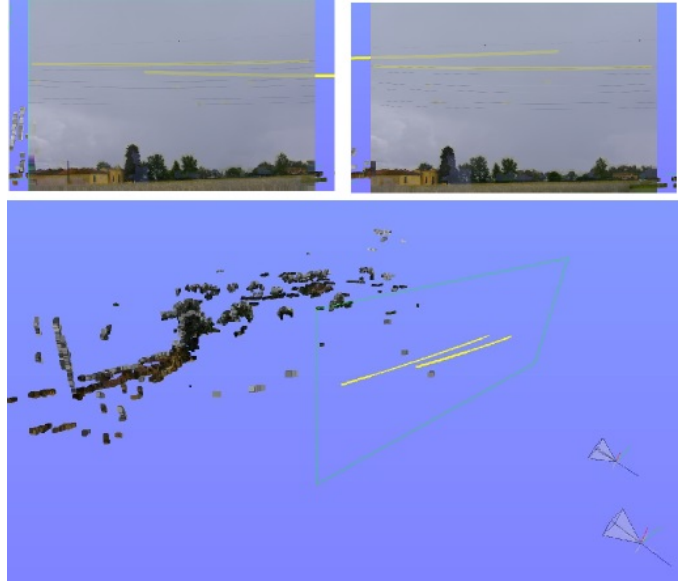


Fig. 2. top: two segmented wires are projected onto a plane  $\theta$ . The two images show the view from the two cameras, respectively. If the camera poses and the plane were exact, the two yellow curve should coincide; bottom: the same scene as seen from a different point of view.

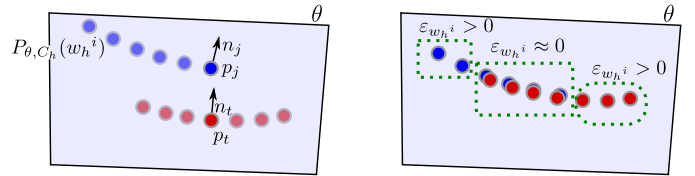


Fig. 3. Left: Calculation of the wire projection error on the plane  $\theta$ . Right: the error function is near 0 only in the overlapping region.

$$\varepsilon_{w_h}(C_h, \theta) = \sum_{\forall j \in P_{\theta, C_h}(w_h)} \frac{focal_h}{\Delta(h, \theta)} \Gamma(p_j, n_j, p_t, n_t)$$

where  $p_j$  is the 3D projection on the plane  $\theta$ ,  $n_j$  the normal with respect to the projected wire,  $p_t$  is the closest point all the other projected wires  $P_{\theta, C_k}(w_k), k \neq h$  and  $n_t$  it is its normal. The distance function  $\Gamma$  is defined as the euclidean distance plus a term that increases exponentially when points with different normal get close to each other [25]:

$$\Gamma(p_j, n_j, p_t, n_t) = \|p_j - p_t\| + \alpha \frac{(1 - n_j \cdot n_t)^\beta}{\|p_j - p_t\| + 1}$$

where the right term of the sum is a function of the angle between the normal, parametrized by  $\alpha$  and  $\beta$ . Its maximum value is reached when two points with opposite normals share the same 3D position and it is equal to  $\alpha 2^\beta$ . In our experiments we obtained the best results by setting  $\alpha$  to the average inter-point distance of points of the same wire on the plane  $\theta$  and  $\beta = 2$ . Finally, the term  $\frac{focal_h}{\Delta(h, \theta)}$  is used to express the error in pixels, with  $focal_h$  the focal distance of the camera  $h$  and  $\Delta(h, \theta)$  the distance of its center of projection from the plane.

Summarizing, the wire projection error is:

$$\varepsilon_W = \sum_{\forall h} \varepsilon_{w_h^i}(C_h, \theta) / \sum_{\forall h} \#w_h$$

where  $\#w_h^i$  is the number of points of the wire  $i$  in the image  $h$ . Please note that the wire projection error can be 0 only if the two portions of the wire are in fact the very same.

### B. Points Reprojection Error

Let  $F = \{f_0, \dots, f_N\}$  the 3D points computed by the SfM pipeline. Each of these points has at least 3 correspondences among the images. The reprojection error of the feature  $i$  is computed by projecting the 3D point onto each image, computing the distance to its 2D feature point and averaging the result:

$$\varepsilon_P(f_i) = \frac{1}{\#Corr_I(i)} \sum_{h \in Corr_I(i)} \|Proj_{C_h}(f_i) - Corr_P(i)\|$$

where  $Corr_I(i)$  is the set of images containing a correspondence, and  $Corr_P(i)$  the 2D correspondence point. However, we are not interested in preserving initial 3D feature points but only to find an equivalent configuration that minimizes the wire reprojection error. Therefore, we replace each feature point  $f_i$  with the 3D point  $f'_i$  minimizing the quadratic distance to the projective lines. In other words we recompute the 3D point cloud in each minimization step.

The contribution of the points reprojection error is then averaged on the number of features  $\#F'$ :

$$\varepsilon_P(C) = \sum_{i \in F'} \frac{1}{\#F'} \varepsilon_P(f'_i)$$

Summarizing, the complete optimization problem for the single wire hypothesis is:

$$\begin{aligned} & \underset{C, \theta}{\text{minimize}} && \varepsilon_W(C, \theta) \\ & \text{subject to} && \varepsilon_P(C) < \varepsilon_S \end{aligned} \quad (1)$$

where  $\varepsilon_S$  is the initial feature reprojection error.

### C. Minimization Setup

The minimization process is carried out by relaxing the constraint in problem 1 and adding it to the objective function:

$$\underset{C, \theta}{\text{minimize}} \quad \varepsilon_W(C, \theta) + \lambda |\varepsilon_S - \varepsilon_P(C)| \quad (2)$$

Please note that here  $\lambda$  determines how much the point reprojection error may be allowed to increase in order to create a consistent 3D reconstruction onto the plane  $\theta$  and it is tuned empirically. In principle we could use the signed value of this error term and maximize the value of the solution of 2 over  $\lambda$  and so obtaining a tight bound for the original problem, that is, we could implement a proper Lagrangian relaxation. Unfortunately, the non-linearity of the error function and the possibly high number of terms over which it is computed (that is, wire points) would make the process very slow and impractical.

Input				Output		
#imgs	#pts	$\varepsilon_P$	$\varepsilon_W$	$\varepsilon_P$	$\varepsilon_W$	time (s)
7	498	27.6	4549	33.5	3106	58
7	498	30.73	20183.55	31.5	16050.54	235
7	498	30.73	20183.55	32.5	17055.54	122
6	494	33.2	4050	40.1	3483	46

TABLE I  
RESULTS FOR  $\lambda = 10$ . DUE TO THE RELAXATION, THE CONSTRAINT ON THE FEATURE PROJECTION ERROR IS NOT RESPECTED BUT THE REPROJECTION ERROR FALLS SENSIBLY, AS IT CAN BE SEEN IN FIGURE 4

### D. Initialization of plane $\theta$

As problem 2 has in general several minima, it is important to set an initial solution which is as much as possible near to the optimal value. Here we use the notion the the photographs are taken along the power line and estimate the plane normal as orthogonal to the line fitting the point of view of the cameras. The offset, that is, the distance of the plane from the cameras, is chosen as half the average value of the distance of the SfM points from the cameras, since in practical those points are almost all further away than the power line (see left side of Figure 4 for an example of estimated plane).

### E. Extension to a generic number of wires

Because the wires in a power line run parallel to each other, extending the formulation to a generic number of wires is trivial. The only change to problem 1 is to turn the objective function to a sum over the wires detected in the images and add one separate offset per wire, so that instead of the parameter  $\theta$  we have  $a, b, d_0, \dots, d_n$  where  $n$  is the number of wires.

## V. RESULTS

We tested our pipeline on real world scenarios. The images of power lines were taken from a height of 1.80mt from the ground and we used few  $6000 \times 4000$  images for each wire section (the portion of wire suspended between two pylons). Table I shows the input data and processing results for two datasets with 7 and 6 images respectively. The algorithm is executed on a PC equipped with Intel I7 Quad Core 3GHz. We use the Newuoa algorithm for unconstrained nonlinear optimization [26].

Since in this phase we did not have access to a ground truth reconstruction of the power lines, we relied on the presence of reconstructed 3D points whose visual feature was also visible on Google Map. We use these correspondences to align the results (camera, plane and 3D points) with the Map and estimate the approximation provided by our method. Figures 4 shows the 3D reconstruction and the 2D superimposition with Google Map. We can see that the resulting plane is fairly well corresponding with the visible power lines but the approximation introduced by using reconstructing point and maps does not allow us to make precise metric statements at this stage. We measured the distances on the same map of Figure 4 and we could see that the actual pylons are 250 mt from each other, our estimation is 7 meters away from the real plane on one side and 12 on the other, while the actual wire is

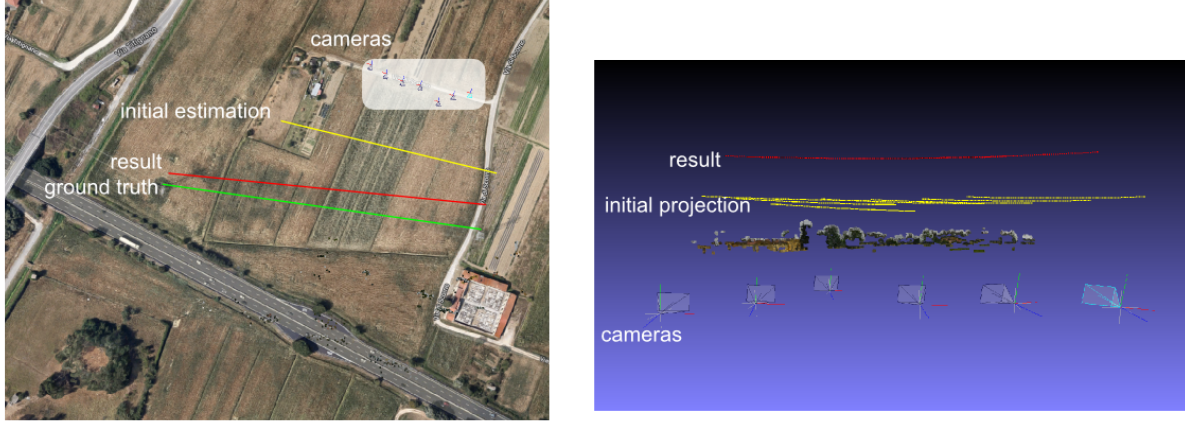


Fig. 4. On the left side we show the superimposition of the result obtained by our algorithm with the aerial view provided by Google Maps. We manually traced the actual wire position with a green segment. The yellow line shows the initial plane estimation computed as in Section IV-E, while the red line is the location of the final plane. On the right, the same dataset as seen from beyond the cameras. Note how the initial projections of segmented wire sections (in yellow) are then aligned in the final configuration (in red).

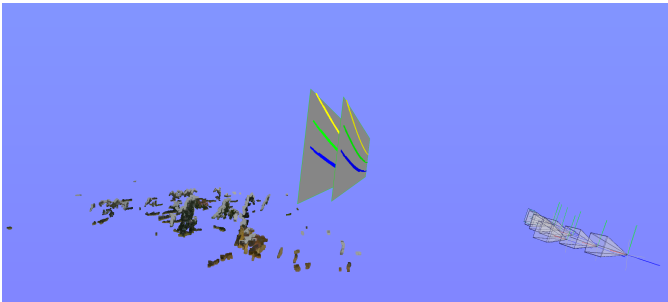


Fig. 5. Result obtained by parameterizing the solution with only two planes (shown as gray rectangles) and assigning the segmented wires to the plane by hand.

105 meters from the closest camera, resulting in a 10% error on depth estimation. Although such estimation cannot be said to be accurate, we should consider it in the light of the fact that the average value of the point reprojection error is very high and make the problem almost undetermined.

The first two rows of Table I are about the same dataset shown in Figure 4. However, the first experiment only considers a single wire (the highest in the segmentation), while the second simultaneously reconstructs all of the 6 wires. As it can be seen from the second line of table I, when optimizing simultaneously for multiple wires we obtain a longer processing time but a smaller average error (per wire). This should not come as a surprise since that more wires means more constraints on camera positions. The third rows also concerns optimization for all the wires but this time we used the knowledge of the wires configuration (three pairs at different heights distributed on two vertical planes) and could

parametrize the target function with only two planes. This is only done to state that we can leverage on the knowledge of type of power lines to define a more ad-hoc parametrization and obtain better results (see Figure 5).

## VI. DISCUSSION AND CONCLUSIONS

Our approach uses assumptions that hold in the particular case of power lines and provides a simple solution to a real problem, in an context where previous solutions to the acquisition of wiry objects could not be applied. We were able to formulate an ad hoc parameterization of the domain of solutions that allowed the problem to be formulated as a simple and elegant minimization problem. On the downside, our approach depends on the success the SfM reconstruction pipeline and of the segmentation process. We performed experiments where the correspondence between wires among images could be determined trivially but this is not always true. It is necessary that we address the problem of making our algorithm resilient to wrong associations of segmented wires, most likely by introducing an outer optimization cycle driven by a RANSAC-like approach. Furthermore, since we use a Lagrangian relaxation approach but cannot afford to maximize the min problem over the  $\lambda$  parameter, it is clear that we are empirically trading camera pose error for consistency of wire projection on the plane  $\theta$ . Our next step is to found this balance automatically without penalizing the running time.

## ACKNOWLEDGMENT

This work was supported by the project SCIADRO, 2016-2019 Regione Toscana PAR FAS 2007-2013.

## REFERENCES

- [1] Y. Jwa, G. Sohn, and H. Kim, "Automatic 3d powerline reconstruction using airborne lidar data," vol. 38, 01 2009.
- [2] B. Guo, Q. Li, X. Huang, and C. Wang, "An improved method for power-line reconstruction from point cloud data," *Remote Sensing*, vol. 8, no. 1, 2016. [Online]. Available: <http://www.mdpi.com/2072-4292/8/1/36>
- [3] R. A. McLaughlin, "Extracting transmission lines from airborne lidar data," *IEEE Geoscience and Remote Sensing Letters*, vol. 3, no. 2, pp. 222–226, April 2006.
- [4] S. Clode and F. Rottensteiner, "Classification of trees and powerlines from medium resolution airborne laserscanner data in urban environments," in *In: Proceedings of APRS Workshop on Digital Image Computing 2005 (WDIC2005)*, 2005.
- [5] L. Zhu and J. Hyppp, "Fully-automated power line extraction from airborne laser scanning point clouds in forest areas," *Remote Sensing*, vol. 6, no. 11, pp. 11 267–11 282, 2014. [Online]. Available: <http://www.mdpi.com/2072-4292/6/11/11267>
- [6] L. Liu, D. Ceylan, C. Lin, W. Wang, and N. J. Mitra, "Image-based reconstruction of wire art," *ACM Trans. Graph.*, vol. 36, no. 4, pp. 63:1–63:11, Jul. 2017. [Online]. Available: <http://doi.acm.org/10.1145/3072959.3073682>
- [7] N. Snavely, S. M. Seitz, and R. Szeliski, "Modeling the world from internet photo collections," *International Journal of Computer Vision*, vol. 80, no. 2, pp. 189–210, Nov 2008. [Online]. Available: <https://doi.org/10.1007/s11263-007-0107-3>
- [8] C. Wu, "Towards linear-time incremental structure from motion," in *2013 International Conference on 3D Vision - 3DV 2013*, June 2013, pp. 127–134.
- [9] S. M. Seitz, B. Curless, J. Diebel, D. Scharstein, and R. Szeliski, "A comparison and evaluation of multi-view stereo reconstruction algorithms," in *2006 IEEE Computer Society Conference on Computer Vision and Pattern Recognition (CVPR'06)*, vol. 1, June 2006, pp. 519–528.
- [10] Y. Furukawa and C. Hernandez, "Multi-view stereo: A tutorial," *Foundations and Trends in Computer Graphics and Vision*, vol. 9, no. 1-2, pp. 1–148, 2015. [Online]. Available: <http://dx.doi.org/10.1561/06000000052>
- [11] M. Hofer, M. Maurer, and H. Bischof, "Improving sparse 3d models for man-made environments using line-based 3d reconstruction," in *2014 2nd International Conference on 3D Vision*, vol. 1, Dec 2014, pp. 535–542.
- [12] R. G. von Gioi, J. Jakubowicz, J. M. Morel, and G. Randall, "Lsd: A fast line segment detector with a false detection control," *IEEE Transactions on Pattern Analysis and Machine Intelligence*, vol. 32, no. 4, pp. 722–732, April 2010.
- [13] M. Hofer, M. Donoser, and H. Bischof, "Semi-global 3d line modeling for incremental structure-from-motion," in *Proceedings of the British Machine Vision Conference*. BMVA Press, 2014.
- [14] M. Hofer, M. Maurer, and H. Bischof, "Line3d: Efficient 3d scene abstraction for the built environment," in *Pattern Recognition*, J. Gall, P. Gehler, and B. Leibe, Eds. Cham: Springer International Publishing, 2015, pp. 237–248.
- [15] V. Litvinov, S. Yu, and M. Lhuillier, "2-manifold reconstruction from sparse visual features," in *2012 International Conference on 3D Imaging (IC3D)*, Dec 2012, pp. 1–8.
- [16] R. Fabbri and B. Kimia, "3d curve sketch: Flexible curve-based stereo reconstruction and calibration," in *2010 IEEE Computer Society Conference on Computer Vision and Pattern Recognition*, June 2010, pp. 1538–1545.
- [17] R. Fabbri and B. B. Kimia, "Multiview differential geometry of curves," *International Journal of Computer Vision*, vol. 120, no. 3, pp. 324–346, Dec 2016. [Online]. Available: <https://doi.org/10.1007/s11263-016-0912-7>
- [18] D. Rao, S. Chung, and S. Hutchinson, "Curveslam: An approach for vision-based navigation without point features," in *2012 IEEE/RSJ International Conference on Intelligent Robots and Systems*, Oct 2012, pp. 4198–4204.
- [19] Z. Li, Y. Liu, R. Walker, R. Hayward, and J. Zhang, "Towards automatic power line detection for a uav surveillance system using pulse coupled neural filter and an improved hough transform," *Machine Vision and Applications*, vol. 21, no. 5, pp. 677–686, Aug 2010. [Online]. Available: <https://doi.org/10.1007/s00138-009-0206-y>
- [20] T. W. Yang, H. Yin, Q. Q. Ruan, J. D. Han, J. T. Qi, Q. Yong, Z. T. Wang, and Z. Q. Sun, "Overhead power line detection from uav video images," in *2012 19th International Conference on Mechatronics and Machine Vision in Practice (M2VIP)*, Nov 2012, pp. 74–79.
- [21] G. Yan, C. Li, G. Zhou, W. Zhang, and X. Li, "Automatic extraction of power lines from aerial images," *IEEE Geoscience and Remote Sensing Letters*, vol. 4, no. 3, pp. 387–391, July 2007.
- [22] J. Oh and C. Lee, "3d power line extraction from multiple aerial images," *Sensors*, vol. 17, no. 10, 2017. [Online]. Available: <http://www.mdpi.com/1424-8220/17/10/2244>
- [23] G. Jkw, B. Vander Jagt, and C. Toth, "Experiments with uas imagery for automatic modeling of power line 3d geometry," vol. XL-1/W4, pp. 403–409, 08 2015.
- [24] C. Wu, S. Agarwal, B. Curless, and S. M. Seitz, "Multicore bundle adjustment," in *CVPR 2011*, June 2011, pp. 3057–3064.
- [25] D. Portelli, F. Ganovelli, M. Tarini, P. Cignoni, M. Dellepiane, and R. Scopigno, "A framework for user-assisted sketch-based fitting of geometric primitives," in *Proceedings of WSCG, the 18th Int. Conference on Computer Graphics, Visualization and Computer Vision*, 2010. [Online]. Available: <http://vcg.isti.cnr.it/Publications/2010/PGTCDS10>
- [26] M. J. D. Powell, *The NEWUOA software for unconstrained optimization without derivatives*. Boston, MA: Springer US, 2006, pp. 255–297.